

Detection of flexural damage stages for RC beams using Piezoelectric sensors (PZT)

Chris G. Karayannis^{1a}, Maristella E. Voutetaki^{2b},
Constantin E. Chalioris^{*1}, Costas P. Providakis^{2c} and Georgia M. Angeli¹

¹Department of Civil Engineering, Democritus University of Thrace, Xanthi, Greece

²Department of Applied Sciences, Technical University of Crete, Chania, Greece

(Received April 11, 2013, Revised September 27, 2013, Accepted March 6, 2014)

Abstract. Structural health monitoring along with damage detection and assessment of its severity level in non-accessible reinforced concrete members using piezoelectric materials becomes essential since engineers often face the problem of detecting hidden damage. In this study, the potential of the detection of flexural damage state in the lower part of the mid-span area of a simply supported reinforced concrete beam using piezoelectric sensors is analytically investigated. Two common severity levels of flexural damage are examined: (i) cracking of concrete that extends from the external lower fiber of concrete up to the steel reinforcement and (ii) yielding of reinforcing bars that occurs for higher levels of bending moment and after the flexural cracking. The purpose of this investigation is to apply finite element modeling using admittance based signature data to analyze its accuracy and to check the potential use of this technique to monitor structural damage in real-time. It has been indicated that damage detection capability greatly depends on the frequency selection rather than on the level of the harmonic excitation loading. This way, the excitation loading sequence can have a level low enough that the technique may be considered as applicable and effective for real structures. Further, it is concluded that the closest applied piezoelectric sensor to the flexural damage demonstrates higher overall sensitivity to structural damage in the entire frequency band for both damage states with respect to the other used sensors. However, the observed sensitivity of the other sensors becomes comparatively high in the peak values of the root mean square deviation index.

Keywords: PZT; Structural Health Monitoring (SHM); Electro-Mechanical Admittance (EMA); Reinforced Concrete (RC); Electro-Mechanical Impedance (EMI); flexural damage; cracking; yielding state; finite element method; Root Mean Square Deviation (RMSD)

1. Introduction

The detection of damaged areas of Reinforced Concrete (RC) structures and further the assessment of their damage severity level are traditionally conducted through in situ inspection including optical examination, X-rays and possible partial uncover of reinforcement. Nevertheless

*Corresponding author, Associate Professor, E-mail: chaliori@civil.duth.gr

^a Professor, E-mail: karayan@civil.duth.gr

^b Ph.D., E-mail: mvoutetaki@yahoo.com

^c Professor, E-mail: cprov@mred.tuc.gr

it is quite obvious that these procedures are time-consuming and most of all they cannot be applied in structural members covered by building materials, in long prestressed concrete bridge beams, in non-accessible members or in foundation elements of structures. The fact that most infrastructural systems worldwide are made of RC in combination with the seismic problem in earthquake prone regions and the observation that these structures age with time and deteriorate as a result of fatigue, overloading and insufficient maintenance necessitate the development of structural health monitoring.

Thus the detection of damages, the assessment of their severity level in non-accessible RC members and even more the on-line monitoring of the possible damage evolution with time are new potentials that probably lie ahead to be investigated based on the properties of the Piezoelectric material lead Zirconate Titanate (PZT).

These challenging fields of study have already become special parts of reinforced concrete and earthquake engineering research that are rapidly developed (Yun *et al.* 2011). Research in these areas can be proven essential in the near future since engineers in seismic-prone regions often face the problem of detecting hidden damage of non-accessible RC members and moreover they have to meet the case of designing intervention works.

A PZT sensor can produce electrical charges when subjected to a strain field and conversely mechanical strain when an electrical field is applied. A theoretical model of the PZT functioning has been proposed by Liang *et al.* (1994). The Structural Health Monitoring (SHM) and damage detection techniques have been developed based on the coupling properties of the piezoelectric materials. The impedance -based SHM approach utilizes the electromechanical impedance of these materials that is directly related with the mechanical impedance of the host structural members, a property that is directly affected by the presence of any structural damage. Thus the impedance extracts and its inverse, the admittance, constitute the properties on which the PZT approach is based for the SHM of reinforced concrete structures. Specifically, the produced effects by the structural damages on the PZT admittance signatures are vertical enlargement or/and lateral shifting of the baseline signatures of the initially healthy structure. These effects are the main damage indicators on for damage detection and evaluation that many researches are based on.

Furthermore statistical techniques and indices have been employed to associate the damage with the observed shifting and alteration in the initial Electro-Mechanical Admittance (EMA) signatures such as the Root Mean Square Deviation (RMSD) (Giurgiutiu and Rogers 1998). Comparison of the effectiveness of the statistical indices have showed that the RMSD is the most robust and representative index for the damage level assessing (Tseng and Naidu 2001, Yang *et al.* 2008) and therefore it is used in the present work.

Sabet Divsholi and Yang (2008) used PZT sensors for the detection of damage location and severity level and Yang *et al.* (2008) used the structural mechanical impedance extracted from the PZT electro-mechanical admittance signature as the damage indicator for the detection of structural damages in a 2-story RC frame. Further, PZT sensors bonded on steel reinforcing bars that were embedded in concrete specimens were also applied in order to perform non-destructive monitoring of the bond development between bar and concrete (Tawie and Lee 2010).

A novel SHM technique using a self-sensing circuit of piezoelectric sensors for detecting debonding between concrete and fibre reinforced polymer sheet laminated to a beam surface has recently been reported by Lee and Park (2012). Debonding levels have been quantified using damage indices extracted from the impedance and guided wave features of the supervised learning-based statistical pattern recognition.

Providakis and Voutetaki (2006) presented a numerical method for SHM and damage

identification of a concrete beam by extracting the Electro-Mechanical Impedance (EMI) characteristics of surface bounded self-sensing PZT patches. The damage was firstly quantified conventionally by the RMSD index and then by using a statistical confidence method in system identification advanced routines of a mathematical computational software.

Further, they extended the aforementioned damage detection - characterization approach and proposed a statistical utilization of EMA using a combination of finite element method and Box-Behnken design of experiment analysis (Providakis and Voutetaki 2007). This technique produces polynomial models that relate damage parameters, such as stiffness reduction, to the EMA signature generated at piezoelectric sensors at specific frequency ranges.

Moreover, a finite element modeling technique for the comparison of active constrained layer damping with purely active damping treatments for suppressing the vibrations of smart structures based on the EMI approach has also been studied (Providakis *et al.* 2008).

Recently, the feasibility of the EMI sensing technique for the online strength gain monitoring of early-age concrete has been investigated and checked with experimental data (Shin and Oh 2009). It was found that the EMI signature is sensitive enough to the strength gain in early age concrete. In the same scope, an innovative active wireless sensing system that consists of a miniaturized EMI measuring chip and a reusable PZT transducer to monitor the concrete strength development at early ages has been proposed (Providakis and Liarakos 2011). The effectiveness of this miniaturized sensing system to monitor the concrete strength during the hydration process has been tested using experimental results of standard cubic concrete specimens.

The aforementioned brief review indicates that the recent developments in piezoelectric materials have inspired researchers to develop new non-destructive evaluation and monitoring methods and techniques in concrete elements.

In this study, the issue of SHM of concrete beams reinforced under flexure with steel bars in the context of the damage index based on the RMSD of electromechanical signatures in time domain response is addressed. The purpose of this investigation is to apply analytical models of admittance based signature data, to analyse their accuracy and validity and check the potential of this technique to become an essential aid in monitoring structural damage in real-time.

The potential of the detection of the flexural damages in the lower part of the mid-span area of a simply supported RC beam using PZTs is analytically examined. The kind of studied damages are very common in flexural concrete beams reinforced with bars located in the low part of the beam where bending tension prevails. Two severity levels of damage are examined in the paper: (i) Flexural cracking of concrete in the middle area of the beam's span that extends from the external lower fibre of concrete up to the steel reinforcing bars. This damage also causes cracks in the interface between concrete and reinforcement resulting this way to full debonding between steel bars and concrete. (ii) For higher levels of bending moment and further to the flexural cracking in the middle area of the beam yielding of the reinforcing bars is also occurred. Yielding of steel causes decrease of the effective diameter of steel bars along the length of the considered area of yielding.

The study includes the application of the finite element method for both healthy and damaged areas. Smeared modeling (Karayannis 2000, Karayannis and Chalioris 2000) is used for cracking and yielded materials. The smeared cracking approach has been realized through the development of constitutive models for the description of cracks in concrete and cementitious materials. Because cracking is a localized phenomenon, severe complications are implied in the establishment of a proper crack model. The smeared crack model is based on the observation that, in reality, concrete cracking consists of systems of parallel cracks that are continuously distributed

over the concrete mass, this model considers the cracks to be adequately represented by parallel micro-cracks distributed (smeared) over the finite elements. That is, cracks are merely represented as a change in the material property of the element over which the cracks are assumed to be smeared. Thus, cracked concrete is represented as an elastic orthotropic material with reduced elastic modulus in the direction normal to the crack plane. With this continuum approach the local displacement discontinuities at cracks are distributed over some tributary area within the finite element and the behaviour of cracked concrete can be represented by average stress-strain relations. This consideration is computationally very convenient and the smeared crack concept fits the nature of the finite element displacement method, since the continuity of the displacement field remains intact and any orientation of the crack propagation direction is allowed. Thus, the method is suitable for the analytical simulation of concrete members using finite element computation schemes (Karayannis 2000).

In this work special attention has been given in the selection of the excitation frequencies. It has been proven that damage detection capability greatly depends on the frequency selection rather than on the level of the excitation loading. This observation demonstrates that excitation loading sequence can have a level low enough that the technique may be considered as applicable and effective for real structures.

2. Electro-Mechanical Admittance (EMA) technique

Recently, the electromechanical admittance, or the inverse of impedance, the so-called EMA technique has received growing attention for in-situ SHM. EMA is an active sensing approach that utilizes PZT as actuators/sensors and its response derives from the dynamic interaction between PZT and the host structure. EMA is typically applied using an electrical impedance analyser which scans a predefined frequency range in the order of tens to hundreds of kHz. The self-sensing feature of a PZT enables transduction of electrical energy to mechanical energy, and vice-versa, between the PZT and the host structure. The electrical admittance of the PZT can be expressed as a coupled equation of mechanical impedance of the actuator and the drive-point mechanical impedance of the host structure (Liang *et al.* 1994).

It is known that damage in the host structure, such as a flexural damage in a RC member, alters the stiffness, damping and mass, which in turn changes the mechanical impedance. The area of a RC beam with flexural cracks has lower stiffness and damping values in comparison to the undamaged concrete areas, whereas the mass of a steel bar is reduced due to yielding in the specific area of inspection. Thus, when a PZT bonded to the structure is actuated, the damage-induced change in the mechanical impedance of the structure is reflected in the electrical admittance of the PZT. When a structure is regularly monitored by extracting the admittance signal to the exciting frequency of the PZT, the changes in this signature become indicative of the presence of structural damage (Sun *et al.* 1995, Naidu and Soh 2004). This way a potential flexural damage can be detected by changes in admittance signatures of smart piezoelectric transducers bonded on the structure.

Further, it is also known that the propagation speed of a wave applied on the piezoelectric transducers (that work as sensors and actuators, simultaneously) is given by $\sqrt{E/\rho}$ where E is the modulus of elasticity and ρ is the density of the material. Thus, when flexural damage occurs the values of E and ρ are modified and consequently the propagation speed and the length of the wave are changed and this way the admittance signal is affected (Wu and Chang 2006).

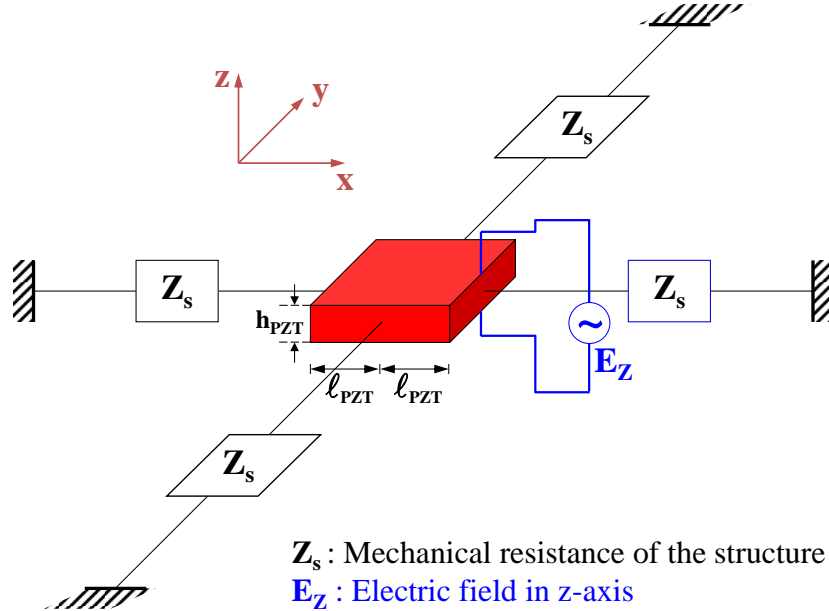


Fig. 1 Model of interaction between PZT and structure

The EMA technique uses piezoelectric materials, such as PZT, which exhibits the characteristic feature to generate surface charge in response to an applied mechanical stress and conversely, undergo mechanical deformation in response to an applied electric field.

Consider a structural component with a PZT patch bonded on it. The related physical model is shown in Fig. 1 for a square PZT patch of length $2l_{PZT}$ and thickness h_{PZT} . When a harmonic voltage $V = V_0 e^{j\omega t}$ is applied in the z-direction, producing an electric field $E = E_0 e^{j\omega t}$, an in-plane vibration is induced in both x and y directions. Liang *et al.* (1994) first modeled the 1-D PZT-structure electro-mechanical interaction, while Bhalla and Soh (2004) and Soh and Bhalla (2005) extended this approach to 2-D structures by using the concept of effective impedance.

The constitutive equations of the PZT patch are (Soh and Bhalla 2005)

$$S_x = \frac{1}{E_{PZT}}(T_x - \nu_{PZT} T_y) + d_{31} E \quad (1a)$$

$$S_y = \frac{1}{E_{PZT}}(T_y - \nu_{PZT} T_x) + d_{32} E \quad (1b)$$

$$D = \bar{\epsilon}_{33}^T E + d_{31} T_x + d_{32} T_y \quad (2)$$

where S_x and S_y are strains, T_x and T_y are stresses, $E = V/h_{PZT}$, V is the input voltage, h_{PZT} is the thickness of the PZT, ν_{PZT} is the Poisson's ratio of PZT, d_{31} and d_{32} are the piezoelectric constants in the x and y directions, respectively, $\bar{\epsilon}_{33}^T = \epsilon_{33}^T(1 - \delta)$ is the dielectric constant at zero stress, δ is

the dielectric loss factor, $j = \sqrt{-1}$, D is the electric displacement and $\bar{E}_{PZT} = E_{PZT}(1 + nj)$ is the elastic modulus at zero electric field where n is the mechanical loss factor.

Considering that the PZT is isotropic on the x-y plane that results in $d_{31} = d_{32}$, the electric displacement in Eq. (2) can be rewritten as

$$D = \bar{\epsilon}_{33}^T E + \frac{d_{31} \bar{E}_{PZT}}{1 - \nu_{PZT}} (u' + v' - 2d_{31} E) \quad (2-s)$$

where $(\cdot)' = \frac{\partial(\cdot)}{\partial x}$ and u and v are the displacements responses in x and y direction, respectively, which can be derived as the solution of the in-plane vibration problem of the PZT patch (Zhou *et al.* 1995)

$$\rho_{PZT} \ddot{u} = \frac{\bar{E}_{PZT}}{1 - \nu_{PZT}^2} u'' \quad (3a)$$

$$\rho_{PZT} \ddot{v} = \frac{\bar{E}_{PZT}}{1 - \nu_{PZT}^2} v'' \quad (3b)$$

where $(\dot{\cdot}) = \frac{\partial(\cdot)}{\partial t}$ and ρ_{PZT} is the density of the PZT patch.

The electric current, I , passing through the PZT patch can be evaluated using the following expression

$$I = j\omega \int_{-\frac{\ell_{PZT}}{2}}^{\frac{\ell_{PZT}}{2}} \int_{-\frac{\ell_{PZT}}{2}}^{\frac{\ell_{PZT}}{2}} D dx dy \quad (4)$$

where ω is the frequency and ℓ_{PZT} is the half length of the PZT.

Further, the Electro-Mechanical Admittance (EMA) of the PZT patch, Y , can be expressed as

$$Y = \frac{I}{V} \quad (5)$$

The technical literature has demonstrated that closed-form expressions for the equations (2) of EMA are only available for simple geometries and structures such as beams (Giurgiutiu and Zagrai 2002), circular-plates (Zagrai and Giurgiutiu 2001) and rectangular thin plates (Zhou and Rogers 1995). In this paper, a finite element methodology is used to extract and analyse the EMA signals.

3. Damage detection by using damage index

A frequency response analysis is performed using the finite element software package COMSOL (2007) and its piezoelectric analysis feature in connection with the enhanced system

identification capabilities of the mathematical package MATLAB (2006). Quantitative damage detection with the EMA method is conventionally achieved by using scalar damage metrics, such as the root mean square deviation non-parametric index

$$RMSD = \sqrt{\frac{\sum_{i=1}^k [\text{Re}(Y_{i,1}) - \text{Re}(Y_{i,2})]^2}{\sum_{i=1}^k [\text{Re}(Y_{i,1})]^2}} \tag{6}$$

where $\text{Re}(Y_{i,1})$ is the real part of the admittance (conductance) of the PZT patch computed at pristine undamaged condition, $\text{Re}(Y_{i,2})$ is the real part of the admittance (conductance) for the “in-question” condition (damage state) as compared with the baseline (pristine) computation at the i^{th} measurement point and k is the number of the measurement points.

The greater the numerical value of the RSMD metric, the larger the difference between the pristine and the “in-question” admittance computation, indicating the presence of damage in the structure.

4. Analytical simulations

The test structure of this study is a simply supported RC beam 1500 mm long with rectangular cross-section 150 mm in width and 150 mm in total depth (or height) with two longitudinal steel bars of 20 mm diameter ($\varnothing 20$). The clear cover of the steel bars is 50 mm. Three PZT patches namely as Sensor-1, Sensor-2 and Sensor-3 are considered to be bonded to the steel bar after a proper flattening of surface in a distance of 785, 655 and 815 mm away from the left end, respectively. This way, Sensor-1 is the closest PZT to the mid-span of the beam (35 mm far to the right) and consequently to the location of the flexural damage of the beam. In the same manner, Sensor-2 is 95 mm far to the left from the mid-span of the beam, whereas Sensor-3 is 65 mm far to the right from the mid-span of the beam and 30 mm away from Sensor-1. The geometry, the reinforcement, the location of the PZT sensors and the mesh of the 3-D model of the RC beam are illustrated in Fig. 2.

The following two flexural damage levels are studied:

(i) Cracking state: Flexural cracking in concrete were simulated in the mid-span of the RC beam specimen by considering cross-width notches 70 mm in depth and 30 mm in width contain softened material (reduced elastic modulus). The damaged area with the first prominent cracks is approached by considering a 90% reduction on the original value of the healthy material modulus of elasticity (smeared crack approach).

(ii) Yielding state: The damage level regarding the yielding state of the bars is also examined in this study. This state is simulated considering a decreased diameter for the steel bars along the length of the yielding area in the mid-span of the beam. Obviously, the flexural cracks described in the cracking state also coexist in the flexural yielding damage state.

The detailed geometry and the mesh of the 3-D models at the mid-span area of the aforementioned damage states of the examined RC beam are displayed in Figs. 3(a) and (b).

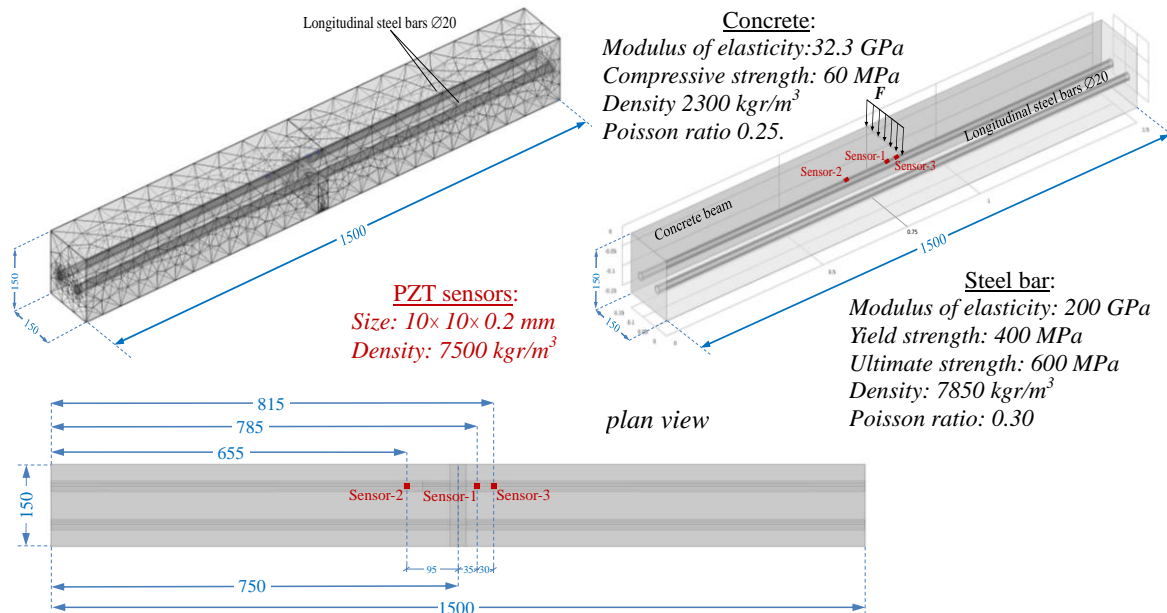
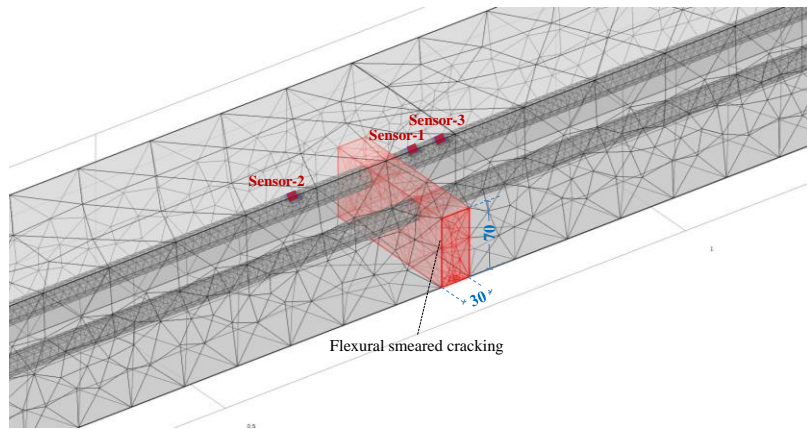


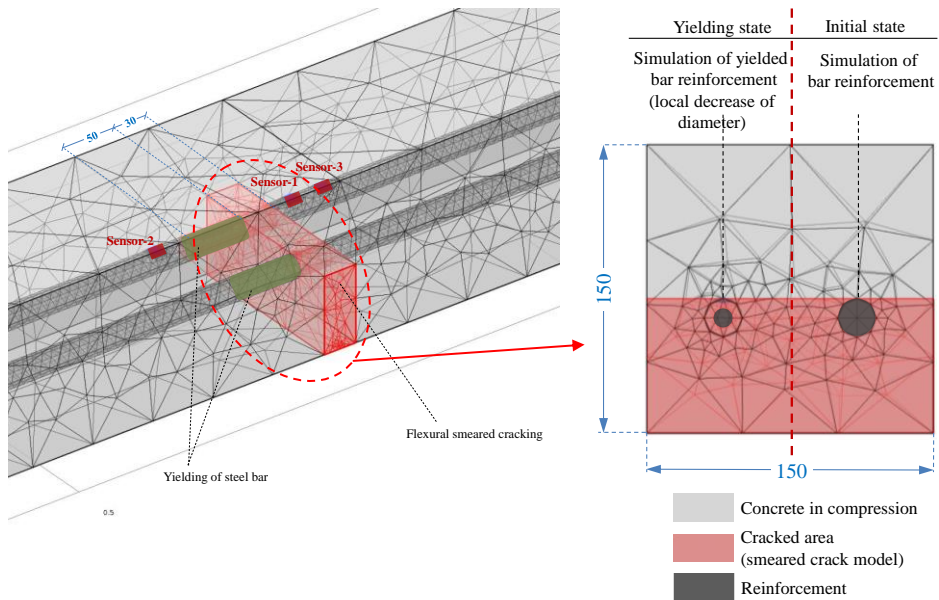
Fig. 2 Geometry, reinforcement, PZT sensors and mesh of the 3-D model of the examined RC beam

The first damage state represents the damage due to the flexural cracking that usually occurs in the middle part of flexural beams while the second state represents the damage state of the reinforced concrete beams after the yielding of the reinforcement due to excessive bending loading. The intention behind simulating the damages in these loading states is to observe the sequential changes of the admittance signatures of the PZT patches regarding the distance from the damage in the two severity levels of structural damage under examination.

It is known that the behaviour of a RC member is greatly affected by the yielding of reinforcing steel due to an imposed flexural loading. Yielding is accompanied by an increase in the flexural deformation of the member due to the simultaneous increase of the local strain of the steel bar. This strain is localized in a disproportionately small region causing necking that leads to a prominent decrease in the local cross-sectional area of the steel bar. This local decrease of the diameter of the yielded longitudinal bar is simulated in the performed finite element analysis as shown in Fig. 3(b). The dense finite element mesh around the yielded reinforcement has been created for good convergence purposes. This was rather expected because the edges of the bar are perfect corners and the finiteness in mesh resolution is a limitation even in high-resolution model, and therefore, as the bar size is further reduced due to necking (yielding), the density of the finite element mesh increases. This fact justifies the different meshing schemes between the yielding and the non-yielding (initial) state of the area around the longitudinal steel bar of the RC beam, as presented in Fig. 3(b).



(a) First damage model: “Flexural cracking”



(b) Second damage model: “Flexural yielding”

Fig. 3 Detailed geometry and mesh of the 3-D models at the mid-span area of the examined damaged states

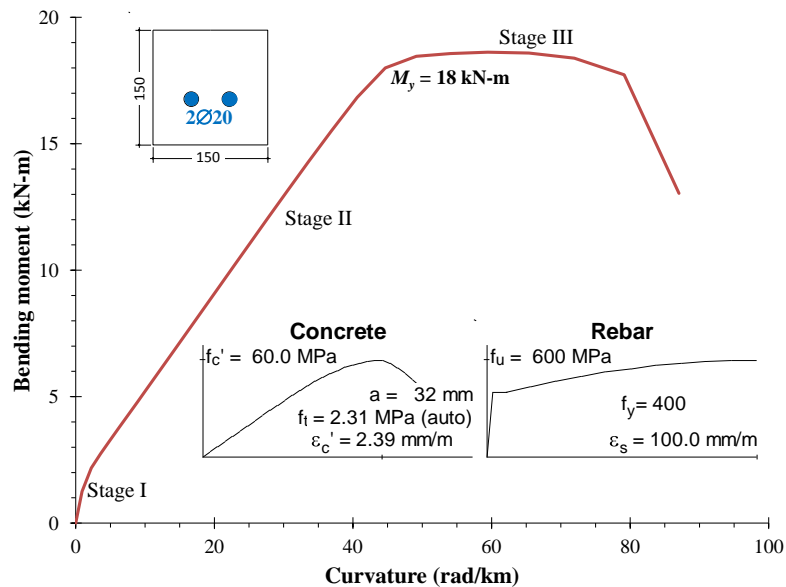


Fig. 4 Calculated flexural behavior of the examined RC beam

It is well-known that the typical flexural behaviour of a RC beam mainly includes the following three stages (Fig. 4). Stage I: the un-cracked part from the beginning till the concrete cracking strength (undamaged element), Stage II: the cracked part up to the yielding strength and Stage III: the post-yielding part till the ultimate strength. The first damage state “flexural cracking” is observed in Stage II, whereas the second damage state “flexural yielding” is observed in Stage III.

The flexural response of the examined RC beam has been calculated with the software package Response-2000 (Bentz and Collins 2000). Fig. 4 displays the bending moment versus curvature curve, the data and the materials properties of the beam. Based on the results of the sectional analysis it is deduced that the flexural strength at yield of the RC beam equals to $M_y = 18$ kN-m that corresponds to an applied load at the mid-span of the beam that equals to 48 kN.

The finite element mesh of the examined cases of the RC beam were generated in COMSOL 3.4a (2007) using approximately 80,000 to 95,000 finite elements depending on the model used and then time domain analyses were performed for a frequency range of 20 to 240 kHz per step of 20 kHz. It is noted that the optimum frequency that provides enough sensitivity for the proper damage detection and repeatability between the measurements is an important parameter that has been investigated herein step. The selection of the appropriate frequency range is a critical issue that depends on the properties of the structural components, the PZT material and the type of damage to be detected (Providakis *et al.* 2013).

The acquisition of the coupled electromechanical impedance has been performed by using four cycles providing a harmonic voltage from 0 to 10 Volts to the PZT patch in time domain range, t , for every central frequency, as described by the following expression

$$V_{PZT}(t) = 10 \sin(2\pi\omega t) \quad (7)$$

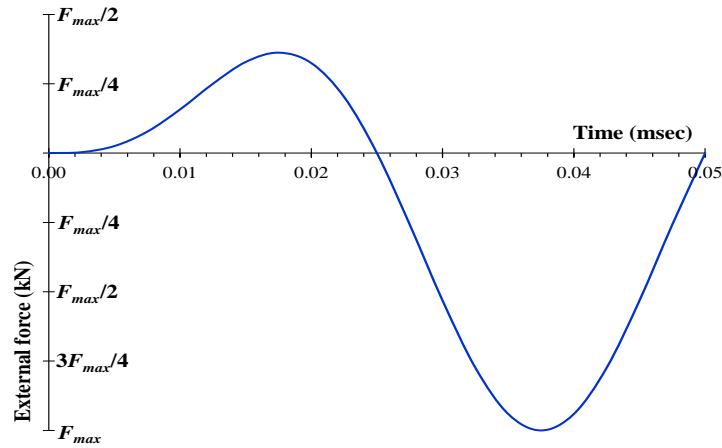


Fig. 5 One cycle of the harmonic external force for the excitation of the beam

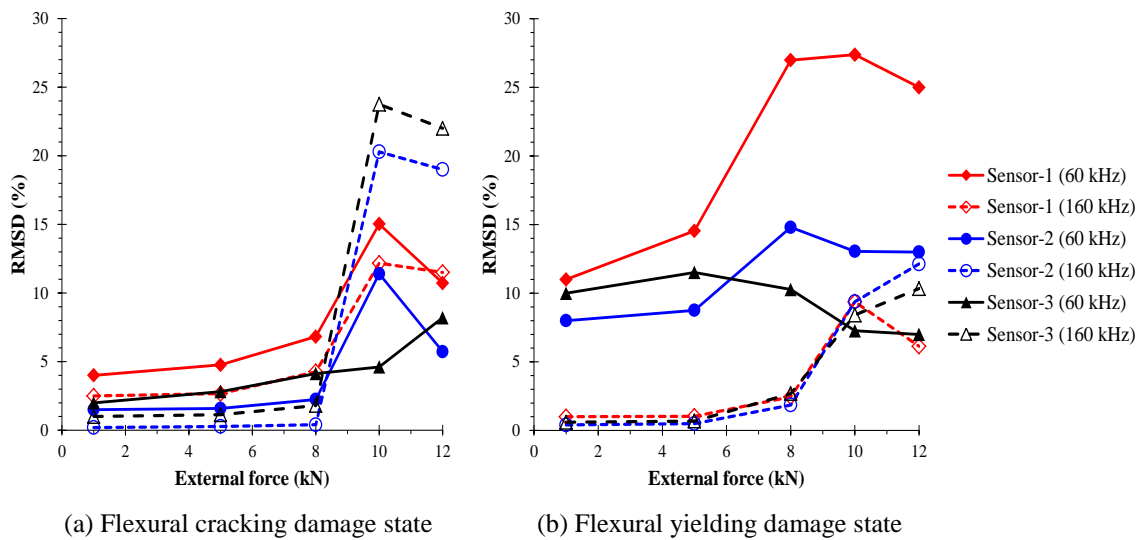


Fig. 6 Influence of the external excitation force level on the RMSD index

In order to numerically evaluate the admittance generated at PZT surface at the predefined frequency range, a fast Fourier transform approach of the time domain excitation signal (external force $[F(t)]$) and COMSOL output response signal (current $[I(t)]$) of the RC beam model has been followed to yield the frequency domain quantities according to Song *et al.* (2008). Based on this conception, the beam is excited by a harmonic external force, F , applied at the mid-span of the beam, modulated with a Hanning window cycle and described by the following relationship (see also Fig. 5)

$$F(t) = F_{\max} 0.5 \left[1 - \cos\left(\frac{2\pi\alpha t}{1.5}\right) \right] \sin(2\pi\alpha t) \tag{8}$$

where F_{max} is the maximum level of applied excitation loading.

It has been observed that the damage detection capability mainly depends on the applied frequency rather than on the loading level of the applied excitation (see also Figs. 6(a) and 6(b)).

In every damage state the real part of the admittance (conductance) was acquired and compared to the pristine (undamaged) state. The pristine state was acquired before the damage states were simulated.

It should be noted that, the existing research in the field of SHM using PZT and EMA technique has recently been developed and the procedure followed till now is based on the comparisons between (a) analytical results of a reference simulation (undamaged or pristine state) and a series of damaged states (Yan *et al.* 2008, Providakis *et al.* 2008, Park *et al.* 2013), or (b) test results of a reference/undamaged specimen and a series of damaged ones (Soh *et al.* 2000, Song *et al.* 2007, Visalakshi *et al.* 2011). Thus, in this study, the analytical results of two flexural damaged states are compared with the corresponding results of a reference/undamaged state, in order to acquire some first concluding remarks. There are several factors that affect the results derived from tests and analyses (such as the size of the examined RC beam, the ratio of the flexural reinforcement, the type of the applied PZT sensors, the type and the degree of the damage, etc). The reproducibility of admittance signals has also been checked in the analytical simulation and the RMSD values derived from the analyses of the pristine and the damage states were the same in each identical frequency response step.

Concerning the influence of the temperature, the findings of existing works indicate that it is an important aspect needing consideration since the properties of PZT are very sensitive to temperature fluctuations (Soh *et al.* 2000). In the study of Sun *et al.* (1995) it has been indicated that a temperature change may cause significant deviation in the signature of the PZT giving a 'false' indication of damage. Generally, increase of temperature causes the decrease in the magnitude of electric impedance and leftward shifting of the real part of the electric impedances (Park *et al.* 2003). A possible solution could be to create a constant temperature environment in the surroundings of the PZT patch, whereby it can be ensured that the temperature remains constant each time the PZT sensor is scanned for the signature acquisition. It is noted that this parameter has not been studied because the temperature was kept constant in all the examined cases since all PZT sensors were bonded in the steel bars that were embedded in the concrete of the beam.

5. Numerical results and discussion

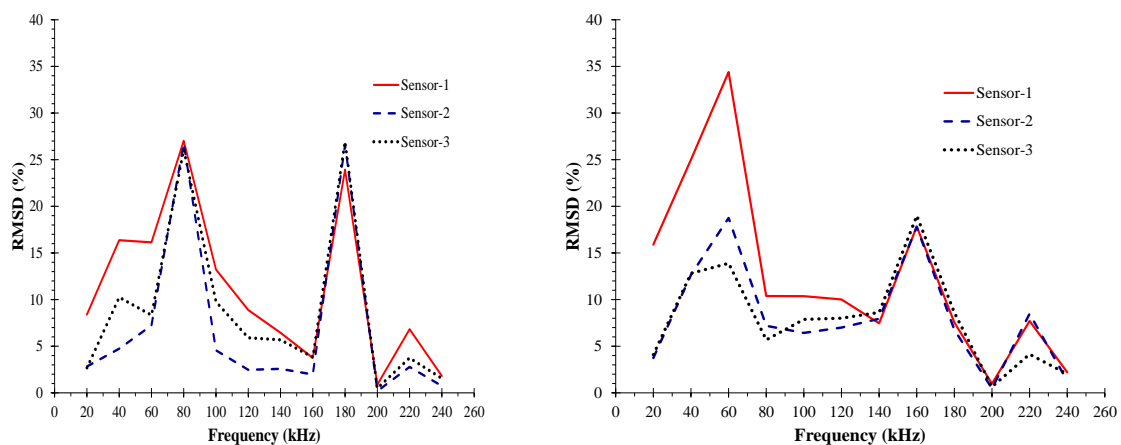
Analyses of the healthy (undamaged) status of the RC beam and the damaged beam with flexural cracking (Stage II, operational level of damage) and with flexural yielding (Stage II) have been performed for various excitation frequencies. For each sub-frequency, the comparison of the admittance response plots for the undamaged with the ones of the damaged beam provides a qualitative approach for damage identification. However, a quantitative assessment of damage could be achieved employing the index RMSD. Figs. 7(a) and 7(b) display the variations in RMSD index value derived from the measurements of the mounted sensors for different sub-frequency intervals between the healthy (pristine state) and the flexural cracking damage state (Fig. 7(a)) and between the healthy and the flexural yielding damage state (Fig. 7(b)).

From Figs. 7(a) and 7(b) it can be deduced that large amplitude differences between the damaged and the undamaged status are recognized for the two excitation levels. Specifically, when excitation frequency is 80 or 180 kHz for the first damage state (cracking) and 60 or 160 kHz for

the second one (yielding) large amplitude differences are detected. Further, it is concluded that the closest PZT patch to the flexural damage (Sensor-1) has satisfactory overall sensitivity to structural damage and demonstrates more or less the higher values of the RMSD index in the entire frequency band for both damage states with respect to the other two sensors. It is also mentioned that Sensor-1 has the ultimate value of RMSD in the case of the flexural yielding damage state and for frequency equal to 60 kHz. Furthermore, the observed sensitivity of Sensor-2 and Sensor-3 is comparable with the sensitivity of Sensor-1 since their RMSD index values approach and occasionally slightly exceed the corresponding values of Sensor-1 in the peaks of the plots. However, Sensor-1 (the closest PZT patch to the flexural damage) seems to be more sensitive in the rather low frequencies (60 and 80 kHz) than in the high frequencies (160 and 180 kHz).

The sensitivity of the EMA technique to detect damage in RC structures depends on several parameters that have not been fully investigated yet. However, an approach of the minimum level of damage, or else a damage threshold, in a specific case could be attempted. In the examined RC beam, a damage threshold can be considered when the cracking area of the concrete has approximately 20% reduction on the original value of the healthy material modulus of elasticity. In this case, based on the measurements of the mounted sensors for different sub-frequency intervals (20-240 kHz) the RMSD index between the healthy and the flexural cracking damage state is very low and therefore this could be assumed as the onset of the damage.

Nevertheless, it should be stressed that this damage threshold only refers to the specific examined conditions. In case that the location of the PZT sensors or the width of the considered smeared crack area changes, then the admittance signature might significantly modified and another damage threshold should be approached. This is attributed to the fact that the size of the considered flexural cracking damage strongly affects the signature acquisition and the effectiveness of the EMA method (Naidu and Soh 2004).



(a) RMSD between the healthy (pristine state) and the flexural cracking damage state (b) RMSD between the healthy (pristine state) and the flexural yielding damage state

Fig. 7 Variations in RMSD index value derived from the measurements of the mounted sensors for different sub-frequency intervals

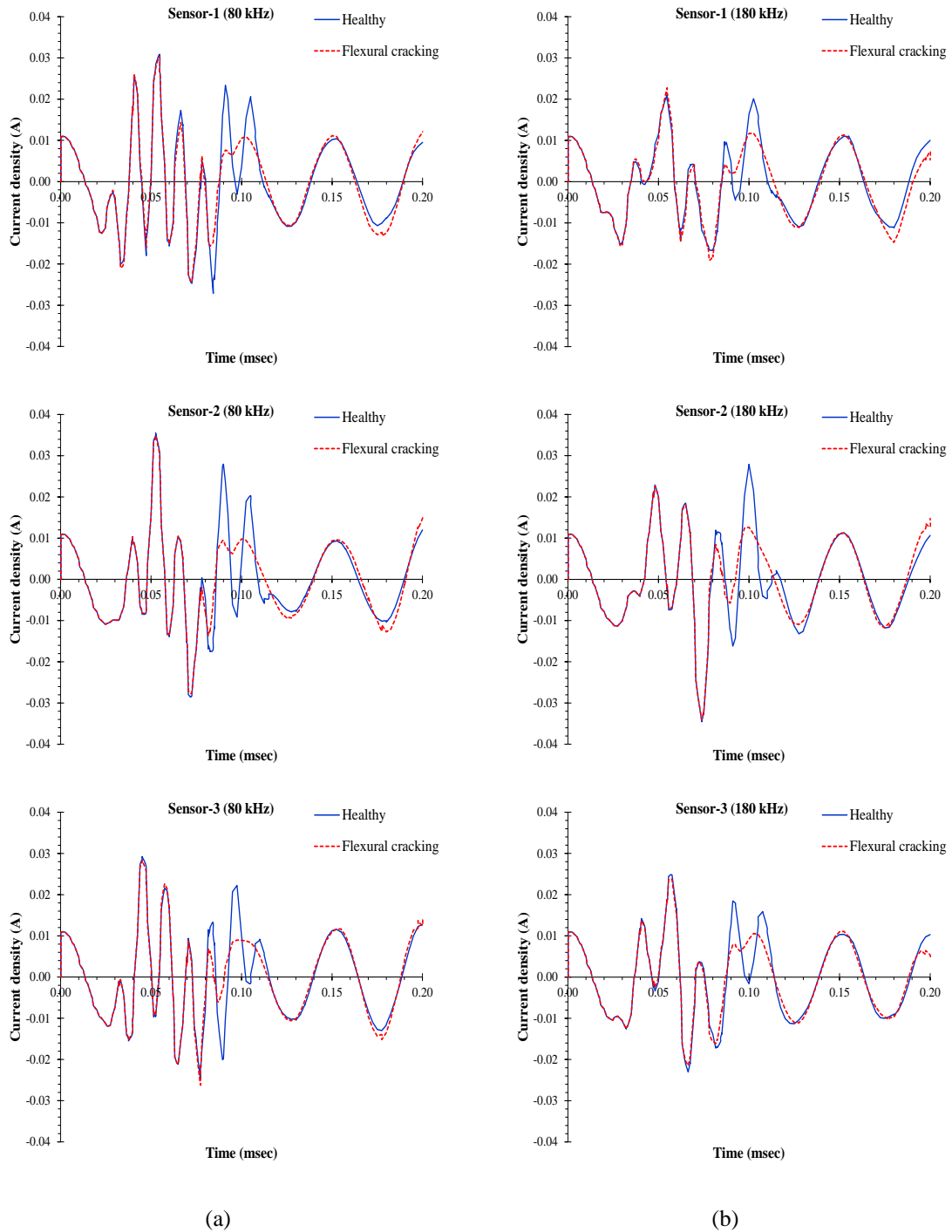


Fig. 8 Current density (in density per PZT area) versus time curves for the healthy and the damaged beam with flexural cracking at the frequency of (a) 80 kHz and (b) 180 kHz

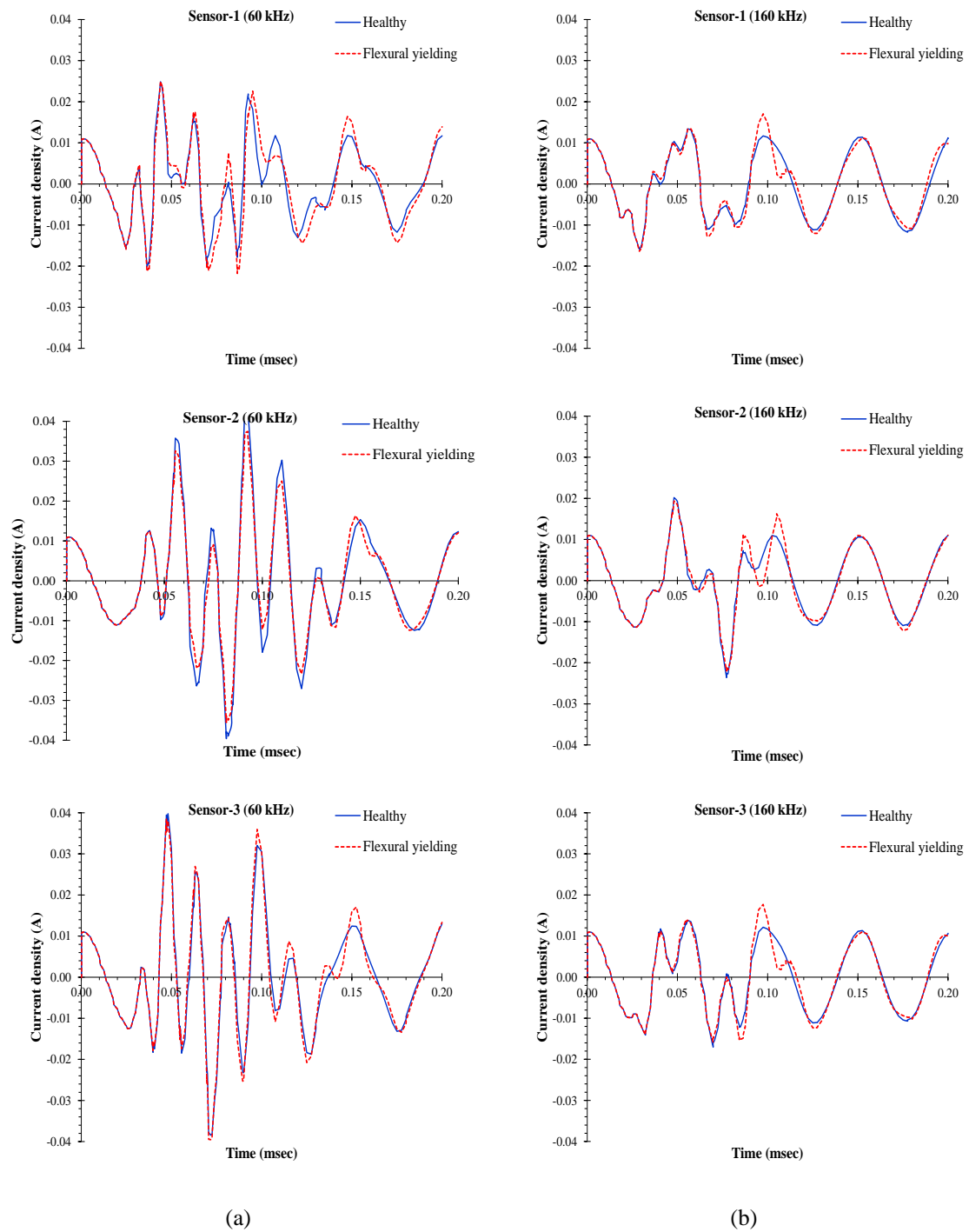


Fig. 9 Current density versus time curves for the healthy and the damaged beam with flexural yielding at the frequency of (a) 60 kHz and (b) 160 kHz

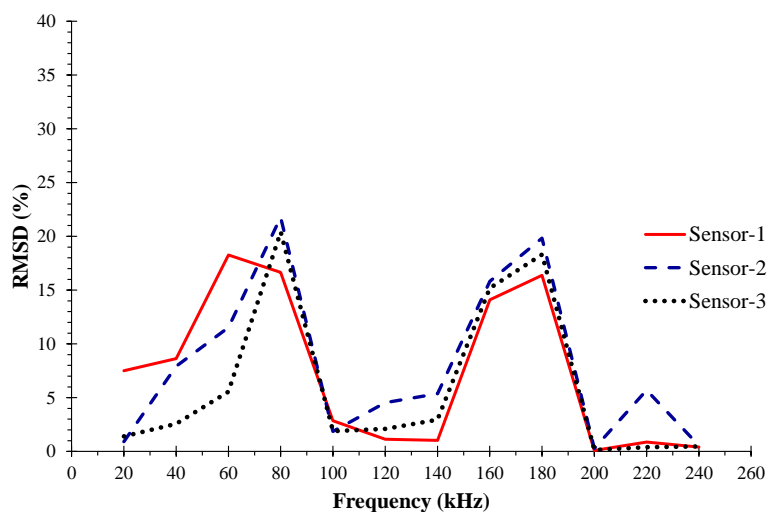


Fig. 10 Variations in RMSD index value between the flexural cracking damage state (pristine state) and the flexural yielding damage state for different sub-frequency intervals

Further, in order to quantify the damage index according to the extent of the damage, analytical results of this paper and from relative existing studies indicated that the known RMSD index can provide a quantitative assessment of the examined flexural damage states. This way, the more severe the damage, the more sensitive the PZT sensor is and therefore, RMSD index increases. And this conclusion coincides with the previous relative studies of PZT sensing based on the damage index techniques.

The sensitivity of the applied PZT sensors is also demonstrated in the current density (in density per PZT area) versus time curves of the healthy and the damaged state for specific frequencies, as illustrated in Figs. 8 and 9 for the flexural cracking and for the flexural yielding, respectively.

The selected frequencies represented in the plots of Figs. 8 and 9 are the frequencies where RMSD index values have been maximised, as shown in Figs. 7(a) and 7(b). Plots of Fig. 8 indicate that the ultimate differences of the current density values between the healthy and the flexural cracking state are observed after the 0.08 msecs and they mainly localised at the time range 0.08-0.13 msecs. In the same manner, the ultimate differences of the current density values between the healthy and the flexural yielding state are observed after the 0.03 msecs (see also plots of Fig. 9). The discrepancies due to the flexural yielding showed in the plots of Fig. 9 are detected in a wider range of time than the corresponding discrepancies due to the flexural cracking state displayed in plots of Fig. 8.

Moreover, the RMSD damage index was plotted for the flexural yielding damage state signatures with respect to the flexural cracking damage state (pristine) signature as shown in Fig. 10. From this Fig. it is deduced that these RMSD index values are considerably lower than the corresponding RMSD index values of Fig. 7b that have derived from the analysis of the healthy and the flexural yielding state, as it was expected. Further, it seems that large amplitude between the examined damaged statuses is recognized when excitation frequency ranges between 60-80 kHz and 160-180 kHz.

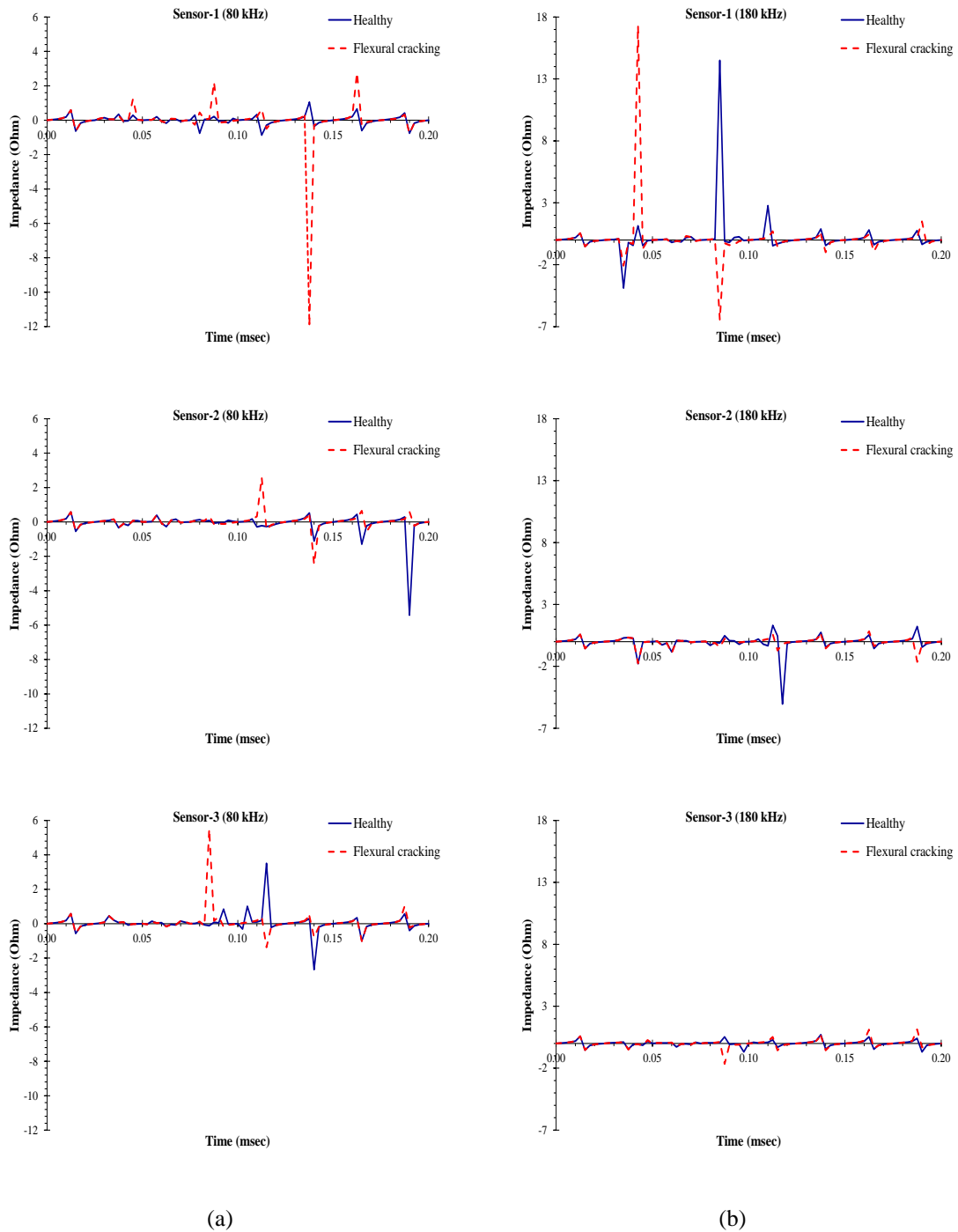


Fig. 11 Impedance versus time curves for the healthy and the damaged beam with flexural cracking at the frequency of (a) 80 kHz and (b) 180 kHz

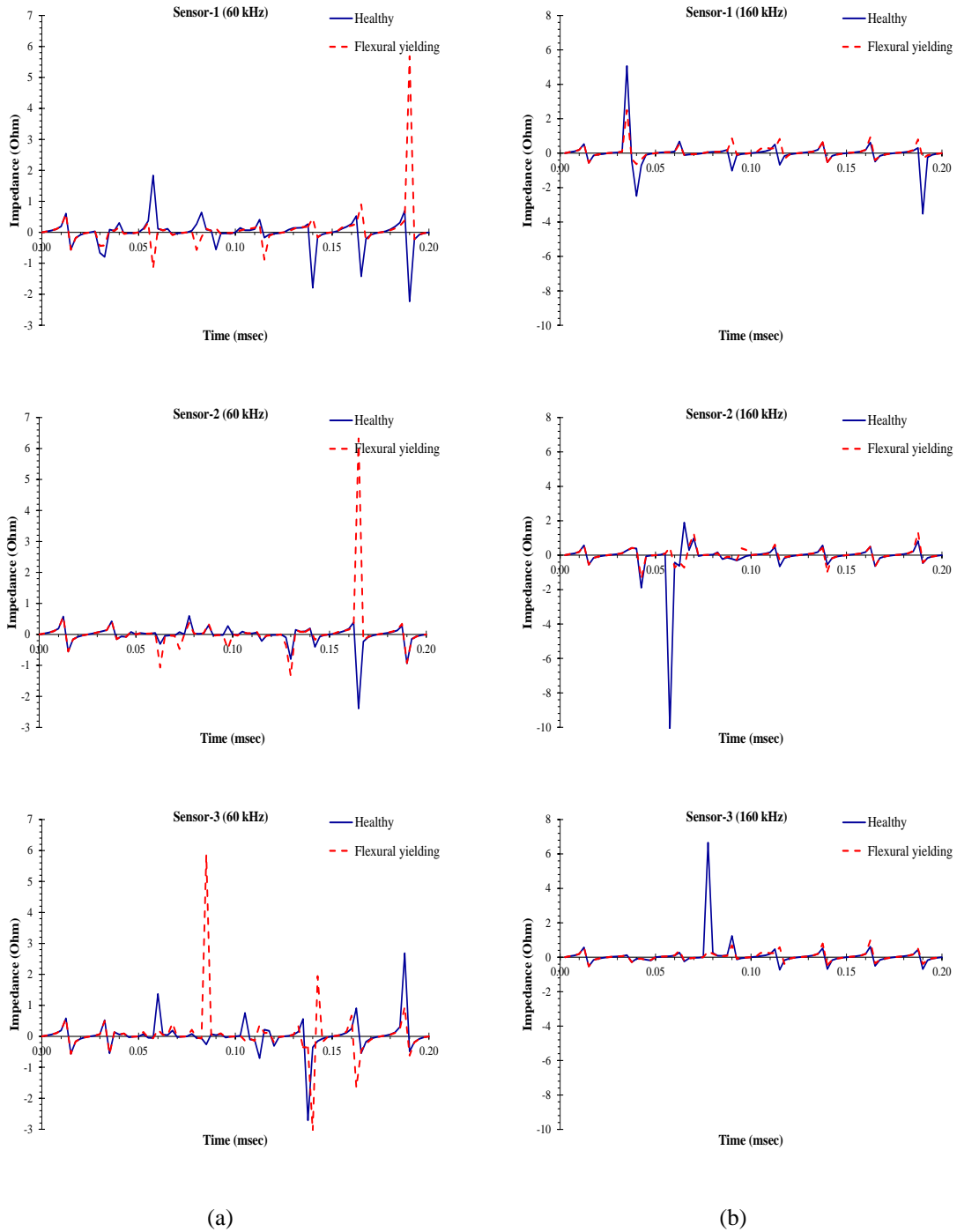


Fig. 12 Impedance versus time curves for the healthy and the damaged beam with flexural yielding at the frequency of (a) 60 kHz and (b) 160 kHz

The impedance versus time curves of the healthy and the flexural cracking state damage for the selected frequencies of 80 and 180 kHz are illustrated in Figs. 11(a) and 11(b), respectively, for each applied PZT sensor. In the same manner, the impedance versus time curves of the healthy and the flexural yielding state damage for the selected frequencies of 60 and 160 kHz are also illustrated in Figs. 12(a) and 12(b), respectively. The plots of Figs. 11(a) and 11(b) confirm that the closest PZT patch to the flexural damage (Sensor-1) has higher sensitivity to the examined flexural cracking damage than the other two sensors, since the plots of Sensor-1 demonstrate higher amplitudes in both frequencies (80 and 180 kHz). Further, Figs. 11 and 12 reveal that the plots of impedance versus time indicate noticeably and more soundly the sensitivity of the applied PZT sensors with respect to the plots of current density versus time showed in Figs. 8 and 9.

As pointed out by Park *et al.* (2006), the sensitivity for damage detection of the EMA method is closely related to the frequency band selected. Based on this concept and in order to select a suitable frequency for acquiring the optimum signature, the PZT sensors are scanned over a wide frequency range of 20–240 kHz as shown in the RMSD versus frequency plots of Fig. 7, for each damage state (flexural cracking and flexural yielding). The RMSD values in these plots show several sharp peaks over a wide range of frequency. Two frequency ranges with the larger amplitude differences are chosen in each state: 80 and 180 kHz for the cracking damage state and 60 and 160 kHz for the yielding damage state. These specific frequencies are applied in order to examine (a) the current density and (b) the impedance time domain response on damage assessment, as presented in Figs. 8 and 9 for the (a) case and in Figs. 11 and 12 for the (b) case. It is also noted that similar methodology has already been followed by Park and Yun (2005) to select a suitable frequency range in an impedance-based damage detection technique using thickness modes of PZT patches for steel structures.

6. Conclusions

The following concluding remarks could be drawn from the research presented herein.

- Special attention has to be given in the selection of the excitation frequencies. It has been proven that damage detection capability greatly depends on the frequency selection rather than on the level of the excitation loading. This observation demonstrates that excitation loading sequence can have a level low enough that the technique may be considered as applicable and effective for real structures.
- The sensitivity for damage detection of the EMA method is closely related to the frequency band selected. Thus, PZT sensors are scanned over a wide frequency range of 20–240 kHz in order to select a suitable frequency for acquiring the optimum signature. This way, two frequency ranges with the larger amplitude differences are chosen in each state: 80 and 180 kHz for the cracking damage state and 60 and 160 kHz for the yielding damage state. These specific frequencies are applied in order to examine the current density and the impedance time domain response on damage assessment.
- The known RMSD index can provide a quantitative assessment of the examined flexural damage states (cracking and yielding) in time domain analyses.
- The closest PZT patch to the flexural damage (Sensor-1) demonstrated higher overall sensitivity to structural damage in the entire frequency band for both damage states with respect to the other two sensors. However, the observed sensitivity of Sensor-2 and Sensor-3

is comparable with the sensitivity of Sensor-1 in the peak values of the RMSD versus frequency plots.

- The sensitivity of the applied PZT sensors can be demonstrated in current density versus time and in impedance versus time plots. The impedance curves indicate more noticeably and soundly the sensitivity of the applied PZT sensors. The discrepancies between the healthy and the flexural yielding state are scattered in a wider range of time than the corresponding discrepancies between the healthy and the flexural cracking state.

Acknowledgments

This research has been co-financed by the European Union (European Social Fund-ESF) and Greek National Funds through the Operational Programme “Education and Lifelong Learning” of the National Strategic Reference Framework (NSRF) - Research Funding Program: THALES. Investing in knowledge society through the European Social Fund.

References

- Bentz, E. and Collins, M.P. (2000), *Response-2000 Reinforced Concrete Sectional Analysis Using the Modified Compression Field Theory*, Version 1.0.5, Software Package, University of Toronto.
- Bhalla, S. and Soh, C.K. (2004), “Structural health monitoring by piezo-impedance transducers I: modelling”, *J. Aerospace Eng.*, **17**(4), 154-165.
- COMSOL 3.4a (2007), *The COMSOL Group*, www.comsol.com, Stockholm, Sweden.
- Giurgiutiu, V. and Rogers, C.A. (1998), “Recent advancements in the electro-mechanical (E/M) impedance method for structural health monitoring and NDE”, *Proceedings of the SPIE, The International Society for Optical Engineering*, **3329**, 536-547.
- Giurgiutiu, V. and Zagari, A.N. (2002), “Embedded self-sensing piezoelectric active sensors for on-line structural identification”, *J. Vib. Acoust.*, **124**(1), 116-125.
- Karayannis, C.G. (2000), “Smearred crack analysis for plain concrete in torsion”, *J. Struct. Eng. - ASCE*, **126**(6), 638-645.
- Karayannis, C.G. and Chalioris, C.E. (2000), “Experimental validation of smearred analysis for plain concrete in torsion”, *J. Struct. Eng. - ASCE*, **126**(6), 646-653.
- Lee, C. and Park, S. (2012), “De-bonding detection on a CFRP laminated concrete beam using self sensing-based multi-scale actuated sensing with statistical pattern recognition”, *Adv. Struct. Eng.*, **15**(6), 919-927.
- Liang, C., Sun, F.P. and Rogers, C.A. (1994), “Coupled electro-mechanical analysis of adaptive material systems - determination of the actuator power consumption and system energy transfer”, *J. Intel. Mat. Syst. Str.*, **7**(1), 12-20.
- MATLAB (2006), *The Mathworks Inc.* U.S. www.mathworks.com, Users Guide.
- Naidu, A.S.K. and Soh, C.K. (2004), “Damage severity and propagation characterization with admittance signatures of piezo transducers”, *Smart Mater. Struct.*, **13**(2), 393-403.
- Park, G., Sohn, H., Farrar, C.R. and Inman, D.J. (2003), “Overview of piezoelectric impedance-based health monitoring and path forward”, *Shock Vib. Dig.*, **35**(6), 451-463.
- Park, I., Kim, S. and Lee, U. (2013), “Dynamics and guided waves in a smart Timoshenko beam with lateral contraction”, *Smart Mater. Struct.*, **22**(7), 075034, 15.
- Park, S., Ahmad, S. and Yun, C.B. (2005), “Health monitoring of steel structures using impedance of thickness modes at PZT patches”, *Smart Struct. Syst.*, **1**(4), 339-353.
- Park, S., Ahmad, S., Yun, C.B. and Roh, Y. (2006), “Multiple crack detection of concrete structures using

- impedance-based structural health monitoring techniques”, *Exper. Mech.*, **46**(5), 609-618.
- Providakis, C.P. and Liarakos, E. (2011), “T-WiEYE: An early-age concrete strength development monitoring and miniaturized wireless impedance sensing system”, *Procedia Eng.*, **10**, 484-489.
- Providakis, C.P. and Voutetaki, M.E. (2006), “Seismic damage detection using smart piezo-transducers and electromechanical impedance signatures”, *Proceedings of the 1st European Conference on Earthquake Engineering and Seismology (1st ECEES)*, Geneva, Switzerland, Paper Number 307.
- Providakis, C.P. and Voutetaki, M.E. (2007), “Electromechanical admittance - Based damage identification using Box-Behnken design of experiments”, *Struct. Durability Health Monit.*, **3**(4), 211-227.
- Providakis, C.P., Kontoni, D.P.N., Voutetaki, M.E. and Stavroulaki, M.E. (2008), “Comparisons of smart damping treatments based on FEM modeling of electromechanical impedance”, *Smart Struct. Syst.*, **4**(1), 35-46.
- Providakis, C.P., Stefanaki, K.D., Voutetaki, M.E., Tsompanakis, J. and Stavroulaki, M.E. (2013), “Developing a multi-mode PZT transducer solution for active-sensing structural health monitoring in concrete structures”, *Proceedings of the 8th IEEE Sensors Applications Symposium (SAS 2013)*, Galveston, Texas, USA.
- SabetDivsholi, B. and Yang, Y. (2008), “Application of PZT sensors for detection of damage severity and location in concrete”, *Proceedings of the SPIE, The International Society for Optical Engineering*, Vol. 7268, art.no. 726813.
- Shin, S.W. and Oh, T.K. (2009), “Application of electro-mechanical impedance sensing technique for online monitoring of strength development in concrete using smart PZT patches”, *Constr. Build. Mater.*, **23**(2), 1185-1188.
- Soh, C.K. and Bhalla, S. (2005), “Calibration of piezo-transducers for strength prediction and damage assessment of concrete”, *Smart Mater. Struct.*, **14**(4), 671-684.
- Song, G., Gu, H. and Mo, Y.L. (2008), “Smart aggregates: multi-functional sensors for concrete structures - a tutorial and a review”, *Smart Mater. Struct.*, **17**(3), doi:10.1088/0964-1726/17/3/033001.
- Song, G., Gu, H., Mo, Y.L., Hsu, T.T.C. and Dhonde, H. (2007), “Concrete structural health monitoring using embedded piezoceramic transducers”, *Smart Mater. Struct.*, **16**(4), 959-968.
- Sun, F.P., Chaudhry, Z., Rogers, C.A., Majmundar, M. and Liang, C. (1995), “Automated real-time structure health monitoring via signature pattern recognition”, *Proceedings of the Smart Structural Materials Conference*, SPIE 2443, 236-247, San Diego, CA, USA.
- Tawie, R. and Lee, H.K. (2010), “Piezoelectric-based non-destructive monitoring of hydration of reinforced concrete as an indicator of bond development at the steel-concrete interface”, *Cement Concrete Res.*, **40**(12), 1697-1703.
- Tseng, K.K.H. and Naidu, A.S.K. (2001), “Non-parametric damage detection and characterization using piezoceramic material”, *Smart Mater. Struct.*, **11**(3), 317-329.
- Visalakshi, T., Bhalla, S. and Bhattacharjee, B. (2011), “Detection and quantification of corrosion using Electro-Mechanical Impedance (EMI) technique”, *Int. J. Earth Sci. Eng.*, **4**, 889-891.
- Wu, F. and Chang, F.K. (2006), “Debond detection using embedded piezoelectric elements for reinforced concrete structures – Part II: analysis and algorithm”, *Struct. Health Monit.*, **5**(1), 17-28.
- Yan, W., Chen, W.Q., Lim, C.W. and Cai, J.B. (2008), “Application of EMI technique for crack detection in continuous beams adhesively bonded with multiple piezoelectric patches”, *Mech. Adv. Mater. Struct.*, **15**(1), 1-11.
- Yang, Y., Hu, Y. and Lu, Y. (2008), “Sensitivity of PZT impedance sensors for damage detection of concrete structures”, *Sensors*, **8**, 327-346.
- Yun, C.B., Lee, J.J. and Koo K.Y. (2011), “Smart structure technologies for civil infrastructures in Korea: recent research and applications”, *Struct. Infrastruct. E.*, **7**(9), 673-688.
- Zagrai, A.N. and Giurgiutiu, V. (2001), “Electro-mechanical impedance method for crack detection in thin plates”, *J. Intel. Mat. Syst. Str.*, **12**, 709-718.
- Zhou, S.W. and Rogers, C.A. (1995), “Power flow and consumption in piezoelectrically actuated structures”, *J. Am. Instit. Aeronaut. Astronaut.* (AIAA), **33**(7), 1305-1311.
- Zhou, S.W., Liang, C.A. and Rogers, C.A. (1995), “Integration and design of piezoceramic elements in

intelligent structures”, *J. Intel. Mat. Syst. Str.*, **6**(6), 733-743.

CC